Electronic Supplementary Information (ESI)

Ultrasensitive water sensors based on fluorenone-tetraphenylethene AIE luminogens

Tao Chen, Ze-Qiang Chen, Wen-Liang Gong, Chong Li* and Ming-Qiang Zhu*

Wuhan National Laboratory for Optoelectronics, College of Optical and Electronic Information, Huazhong University of Science and Technology, Wuhan, Hubei 430074, P.R. China.

E-mail: chongli@hust.edu.cn; mqzhu@hust.edu.cn.

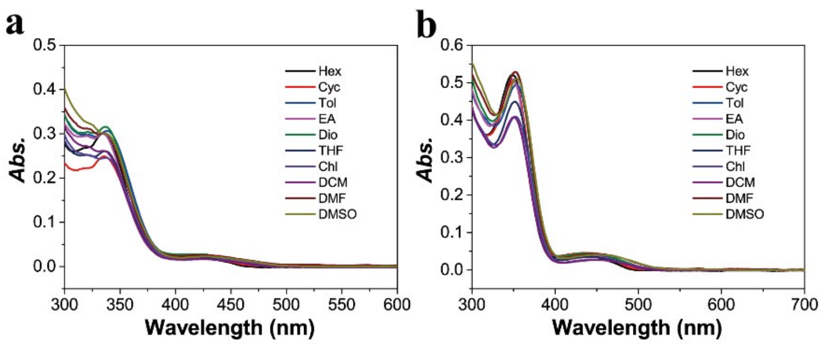

Fig. S1 Absorption spectra of (a) TPE-FO and (b) TPE-FO-TPE in various solvents.

Table S1. Optical properties of TPE-FO and TPE-FO-TPE in various solvents.

Solvents	Δf	TPE-FO		TPE-FO-TPE	
		λ_{Em} /nm	Φ_F	λ_{Em} /nm	Φ_F
Hex	-0.001	504	0.211	530	0.364
CyHex	-0.002	506	0.229	532	0.353
Tol	0.013	528	0.198	528	0.195
EA	0.200	534	0.199	554	0.206
Dio	0.022	530	0.227	558	0.186
THF	0.210	532	0.226	556	0.226
Chl	0.148	582	0.017	602	0.146
DCM	0.217	584	0.023	592	0.033
DMF	0.274	594	0.004	582	0.060
DMSO	0.263	/	0.000	592	0.017

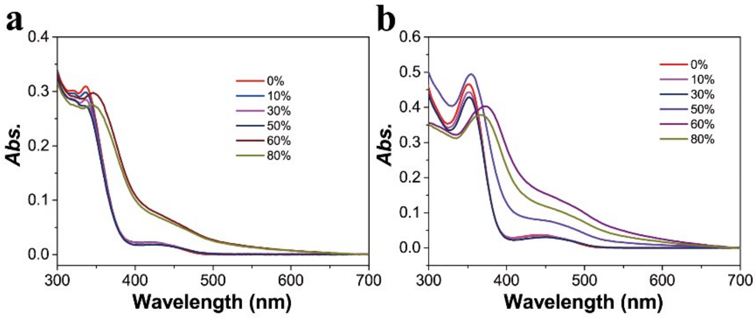

Fig. S2 Absorption spectra of (a) TPE-FO and (b)TPE-FO-TPE in DMSO/water mixtures with different water contents.

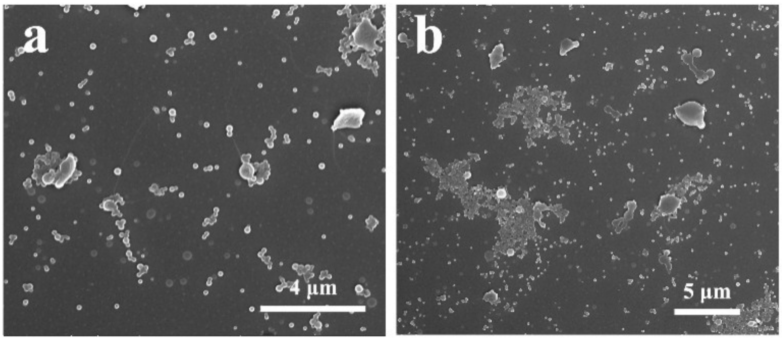

Fig. S3 SEM images of (a) TPE-FO (b) TPE-FO-TPE in DMSO/water mixtures with 60% water fraction.

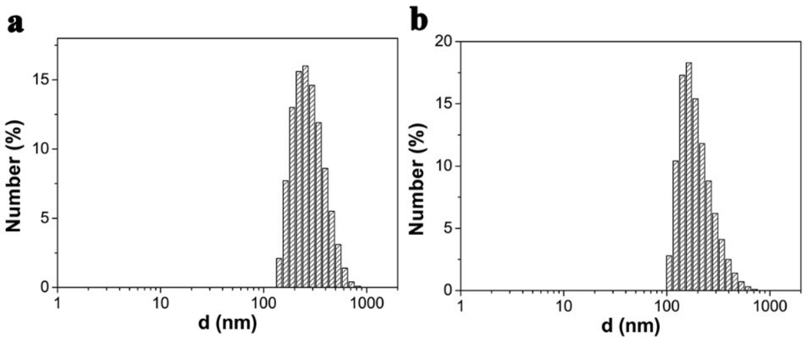

Fig. S4 Hydrodynamic diameter distributionin of TPE-FO (a) and TPE-FO-TPE (b) in DMSO/water mixtures with 60% water fraction.

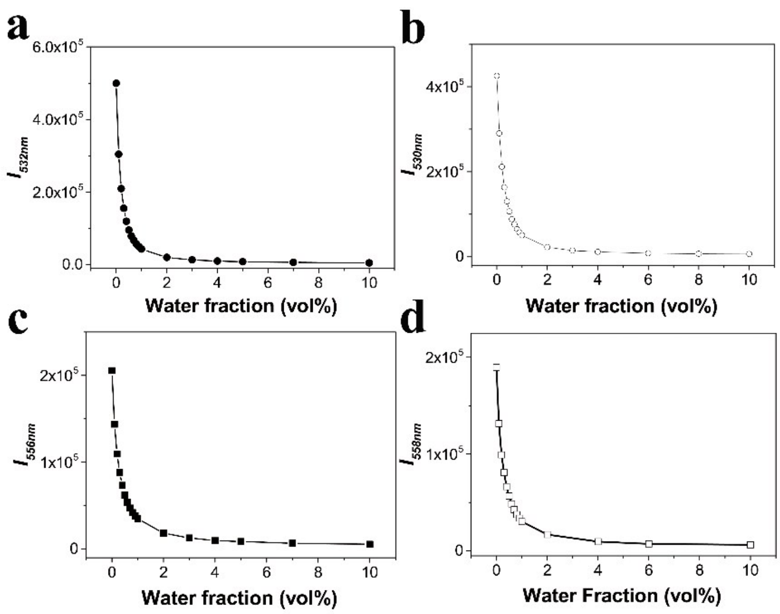

Fig. S5. Changes in PL peak intensities of(a) TPE-FO in THF, (b) TPE-FO in dioxane, (c) TPE-FO-TPE in THF and (d) TPE-FO-TPE in dioxane in the presence of increasing amount of water (0 to10%, vol).

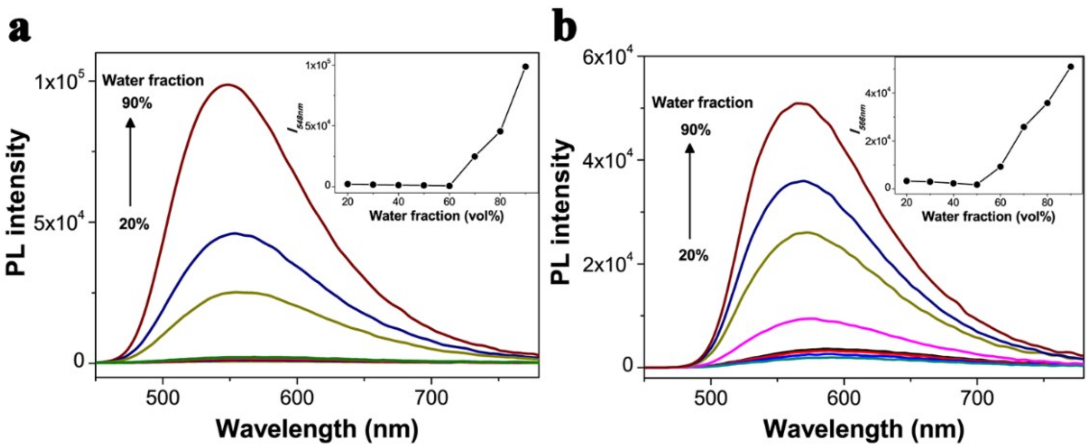

Fig. S6 Fluorescence spectrums of TPE-FO (a) and TPE-FO-TPE (b) in THF-water mixture containing high water fraction. Insets show the plot of the fluorescence intensity versus water fraction at 548 and 560 nm for TPE-FO (a) and TPE-FO-TPE (b), respectively. The concentration is 10 nM. The excitation wavelength is 360 nm.

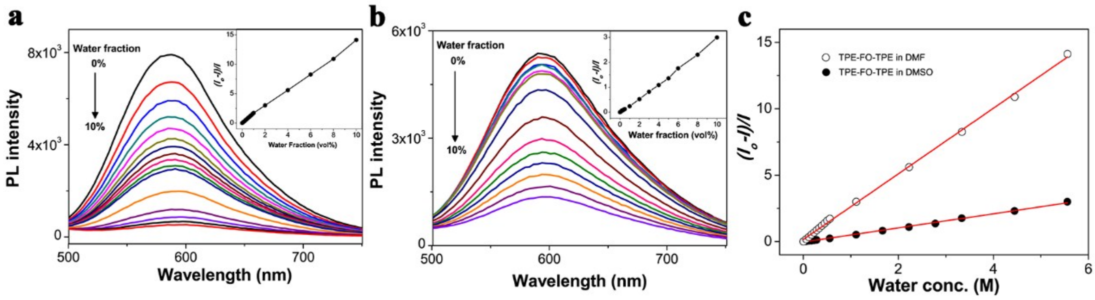

Fig. S7 Fluorescence spectra of TPE-FO-TPE with the increasing water fraction in DMF (a) and DMSO (b) (Concentration 10 nM, excitation at 360 nm). (c) The Stern–Volmer plot of (Io-I)/I versus water concentration (M), where Io and I represent the peak intensity in the absence and in the presence of water, respectively. The red curves represent the linear fitted curves.

Table S2 Comparison of the detection limit of fluorenone-tetraphenylethene compounds with previously reported fluorescent water sensors in THF.

Detection limit (ppm)	Compound	Sensing strategy	Ref.
1125 (0.1%)	1	PET	1
4498 (0.4%)	2	PET	2
2249 (0.2%)	3	PET	3
157 (0.014%)	4	PET	4
90 (0.008%)	5	PET	5
67 (0.006%)	6	ESIPT	6
798 (0.071%)	7	Water as a competitive ligand	7
7085 (0.63%)	8		
34 (0.003%)	9	Water as a competitive ligand	8
495 (0.0464%)	10	Chemical reaction	9
37 (0.0033%)	11	Chemical reaction	10
3374 (0.3%)	12	Hydrogen-bond interactions	11
11021 (0.98%)	13		
22 (0.002%)	14	Hydrogen-bond interactions	12
33 (0.003%)	15		
25 (0.0022%)	16	ICT and Hydrogen-bond interactions	13
36 (0.0032%)	17		
225 (0.02%)	18	ICT	14
663 (0.059%)	19	ICT	15
112 (0.01%)	20	ICT	15
63 (0.0056%)	21	ICT and AIEE	17
109 (0.0097%)	22		
112 (0.01%)	23	ICT and AIEE	18
56 (0.005%)	24	ICT and AIEE	19
11 (0.0010%)	TPEFO	ICT and Hydrogen-bond interactions	This work
14 (0.0014%)	TPE-FO-		

TPE

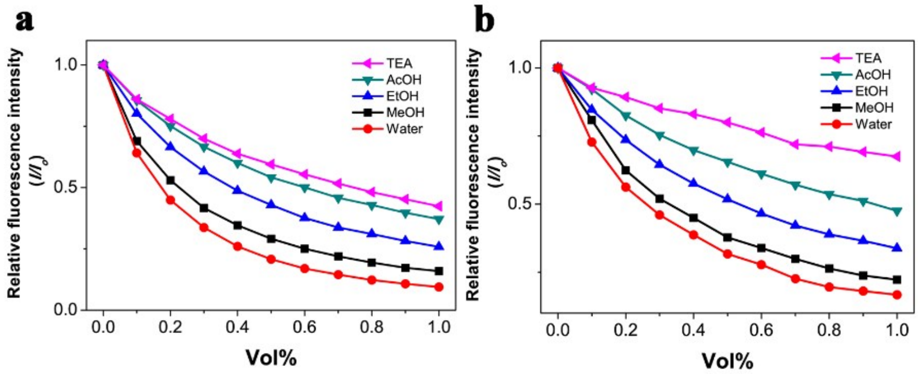

Fig. S8 Relative peak fluorescence intensity of TPE-FO (a) and TPE-FO-TPE (b) in THF in the presence of increasing amount of analyte. TEA, triethylamine; AcOH, acetic acid; EtOH, ethyl alcohol; MeOH, methanol.

Table S3. HOMO and LUMO energy levels and HOMO-LUMOenergy gaps of TPE-FO and TPE-FO-TPE calculated using B3LYP/6-31G(d) basis set.

	TPE-FO	**TPE-FO-TPE**
LUMO /ev	-2.24	-2.25
HOMO /ev	-5.31	-5.23
ΔE /ev	3.07	2.98

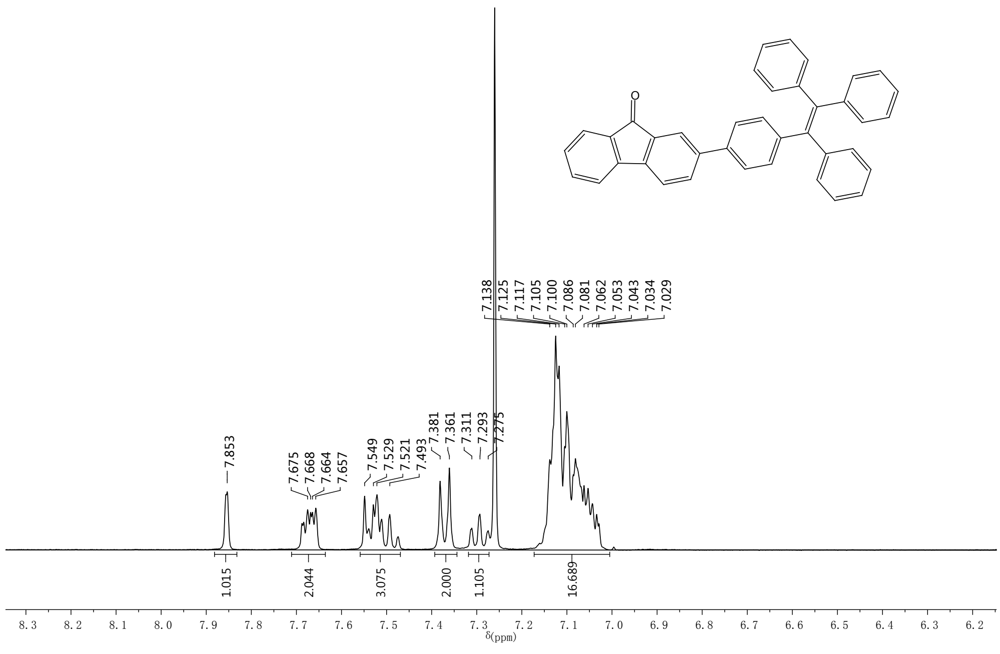

Fig. S9. ^{1}H NMR spectra of TPE-FO.

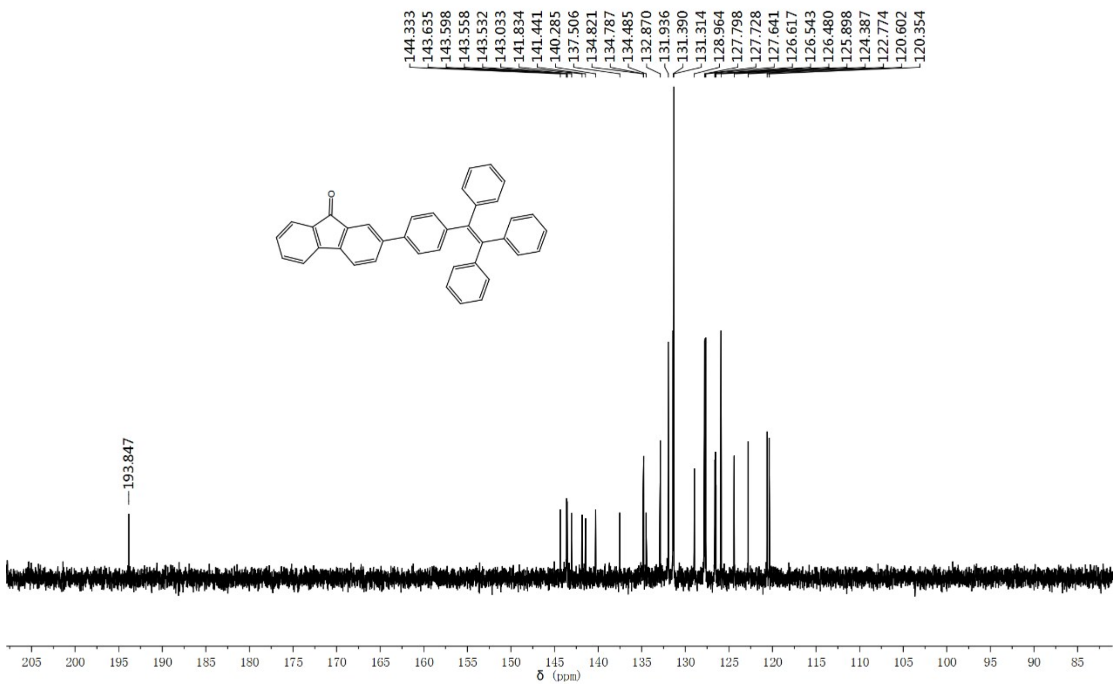

Fig. S10. ^{13}C NMR spectra of TPE-FO.

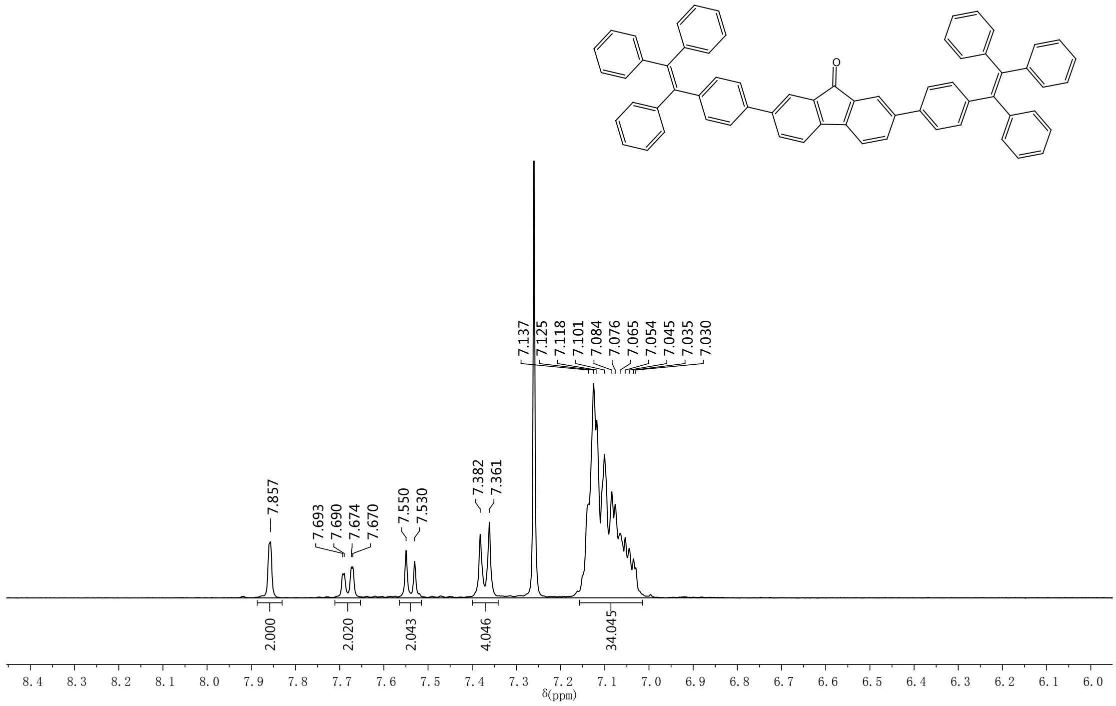

Fig. S11. ^{1}H NMR spectra of TPE-FO-TPE.

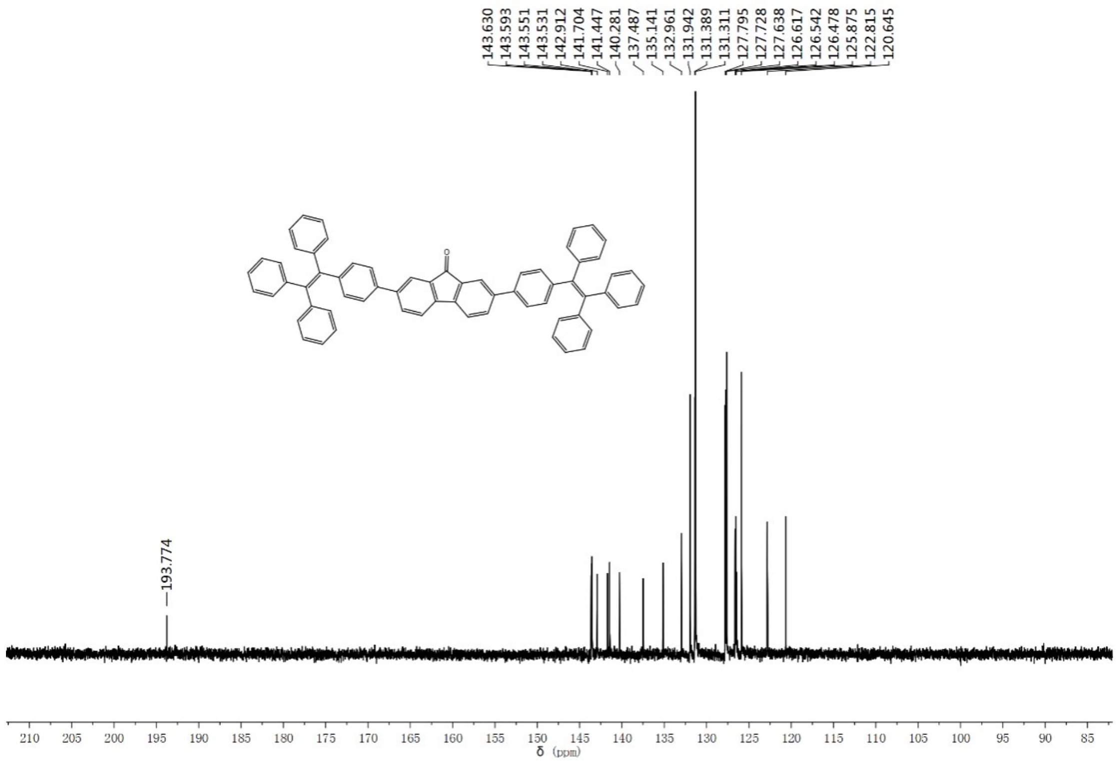

Fig. S12. ^{13}C NMR spectra of TPE-FO-TPE.

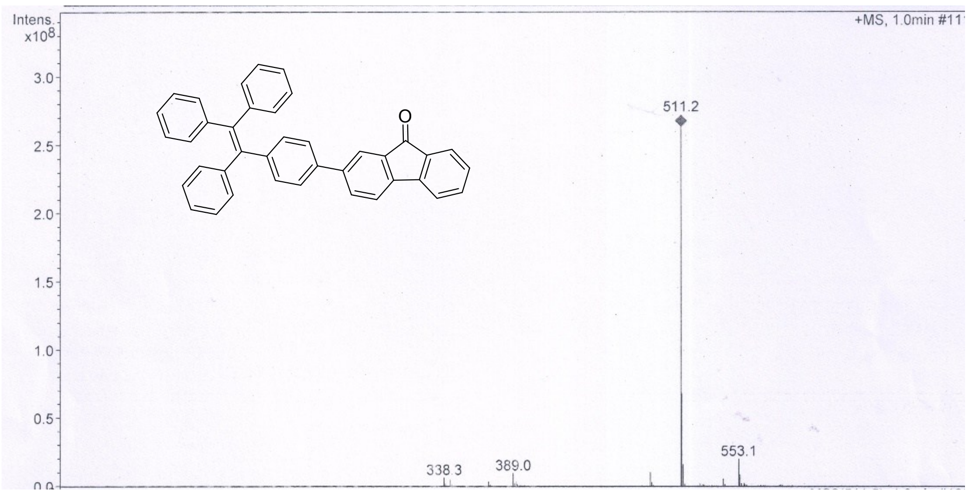

Fig S13. MS spectra of TPE-FO

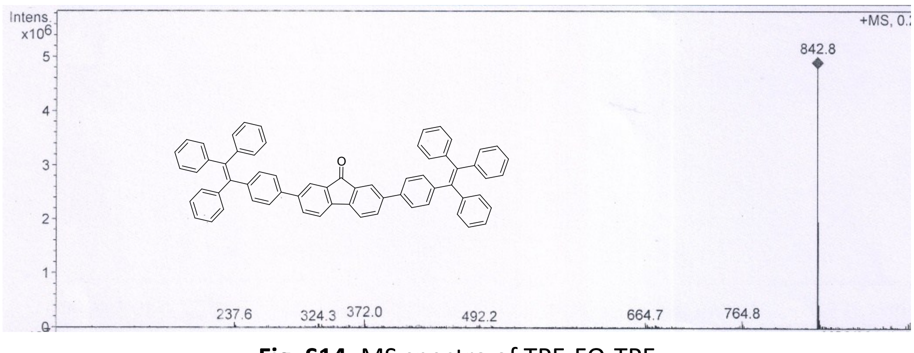

Fig. S14. MS spectra of TPE-FO-TPE

References

1 Y. Ooyama, M. Sumomogi, T. Nagano, K. Kushimoto, K. Komaguchi, I. Imae and Y. Harima, *Org. Biomol. Chem.*, 2011, **9**, 1314.

2 Y. Ooyama, A. Matsugasako, T. Nagano, K. Oka, K. Kushimoto, K. Komaguchi, I. Imae and Y. Harima, *J. Photochem. Photobiol. A*, 2011, **222**, 52.

3 Y. Ooyama, A. Matsugasako, K. Oka, T. Nagano, M. Sumomogi, K. Komaguchi, I. Imae and Y. Harima, *Chem. Commun.*, 2011, **47**, 4448.

4 Y. Ooyama, A. Matsugasako, Y. Hagiwara, J. Ohshita and Y. Harima, *RSC Adv.*, 2012, **2**, 7666.

5 Y. Ooyama, K. Furue, K. Uenaka and J. Ohshita, *RSC Adv.*, 2014, **4**, 25330.

6 J. S. Kim, M. G. Choi, Y. Huh, M. H. Kim, S. H. Kim, S. Y. Wang and S.-K. Chang, Bull. *Korean Chem. Soc.*, 2006, **27**, 2058.

7 Y. H. Kim, M. G. Choi, H. G. Im, S. Ahn, I. W. Shim and S.-K. Chang, *Dyes Pigm.*, 2012, **92**, 1199.

8 P. Kumar, R. Kaushik, A. Ghosh and D. A. Jose, *Anal. Chem.*, 2016, **88**, 11314-11318.

9 G. Men, G. Zhang, C. Liang, H. Liu, B. Yang, Y. Pan, Z. Wang and S. Jiang, *Analyst*, 2013, **138**, 2847.

10 S. Pal, M. Mukherjee, B. Sen, S. Lohar and P. Chattopadhyay, *RSC Adv.*, 2014, **4**, 21608.

11 S. Cha, M. G. Choi, H. R. Jeon and S.-K. Chang, *Sens. Actuators, B*, 2011, **157**, 14.

12 D. Citterio, K. Minamihashi, Y. Kuniyoshi, H. Hisamoto, S.i. Sasaki, K. Suzuki, *Anal. Chem.*, 2001, **73**, 5339.

13 Z. Li, Q. Yang, R. Chang, G. Ma, M. Chen and W. Zhang, *Dyes Pigm.*, 2011, **88**, 307.

14 L. Ding, Z. Zhang, X. Li and J. Su, *Chem. Commun.*, 2013, **49**, 7319-7321.

15 X. L. Guan, T. M. Jia, D. H. Zhang, Y. Zhang, H. C. Ma, D. D. Lu, S. J. Lai and Z. Q. Lei, *Dyes Pigm.*, 2017, **136**, 873-880.

16 M. Tanioka, S. Kamino, A. Muranaka, Y. Shirasaki, Y. Ooyama, M. Ueda, M. Uchiyama, S. Enomoto and D. Sawada, *Phys. Chem. Chem. Phys.*, 2017, **19,** 1209-1216.

17 Y. Zhang, D. Li, Y. Li, J. Yu, *Chem. Sci.*, 2014, **5**, 2710.

18 W. Chen, Z. Zhang, X. Li, H. Ågren and J. Su, *RSC Adv*., 2015, **5**, 12191.

19 L. Wang, L. Yang, L. Li and D. Cao, *New J. Chem.,* 2016, **40**, 6706-6713.